Phi: Jurnal Pendidikan Fisika dan Terapan
Vol.12 No.1 (2026) 16-32
ISSN: 2460-4348, e-ISSN: 2549-7162
https://jurnal.ar-raniry.ac.id/index.php/jurnalphi/index

Article Type: *original research*

Identification of Agricultural Suitability Zones and Groundwater Contamination Using Geoelectrical and Soil Physicochemical Analysis in Sukasari Village, West Java, Indonesia

Salma Salsadila[1], Silvia Dahayu Santoso[1], Nashifa Karisma Khanri[1], Difa Mutafawwiqoh[1], Okan Jonathan Hutasoit[1], Dwi Santi Lestari[1], Arief Rahman Hakim Ritonga[1], Kartika Hajar Kirana[1], Dini Fitriani[1], Eleonora Agustine[1]

[1]Department of Geophysics, Faculty of Mathematics and Natural Sciences, Universitas Padjadjaran, Sumedang, West Java, Indonesia

Correspondence E-mail: eleonora.agustine@unpad.ac.id

ARTICLE INFO

Article History:
Received: 13 September 2025
Revised: 28 November 2025
Accepted: 1 January 2026
Published: 4 January 2026

Keywords:
Agricultural; Anthropogenic; Geoelectrical; Physicochemical; Pollution; Soil Sample;

ABSTRACT

Soil and groundwater pollution from anthropogenic activities poses a significant challenge to agricultural sustainability in rural areas, including Sukasari Village, Tanjungsari District, Sumedang Regency. This study aims to delineate contaminated zones and characterize contaminant distribution patterns through the integration of geoelectrical methods and soil physicochemical analysis. The geoelectrical survey was conducted along eight lines using a 48 electrode configuration with 1 meter spacing. The resistivity cross-sections revealed high-resistivity anomalies in the garden area located downslope of the settlement, indicating contaminant accumulation. This finding was supported by soil test results that confirmed the presence of pollutants, while the area around the biodigester remained relatively uncontaminated. The results indicate that the primary sources of contamination are household and agricultural activities in the southern settlement area, with contaminant migration toward the gardens and rice fields in the north. Overall, this study demonstrates that integrating geoelectrical methods and soil physicochemical analysis is an effective approach for mapping subsurface contamination and supporting sustainable agricultural land management.

1. INTRODUCTION

The agricultural sector is a strategic sector that plays a crucial role in supporting the economy and ensuring food security, particularly in rural areas such as Sukasari Village. The sustainability of this sector is strongly influenced by land conditions and the availability of adequate groundwater resources. However, increasing anthropogenic activities, such as the intensive use of chemical fertilizers, unsustainable agricultural practices, and domestic waste disposal, have led to land degradation and groundwater pollution, thereby threatening agricultural productivity (Brontowiyono et al., 2022; Yusuf

et al., 2023). Addressing these challenges requires an integrated scientific approach capable of providing accurate information on subsurface conditions as a basis for sustainable natural resource management.

Geophysical methods, particularly the geoelectric method, have proven effective in mapping subsurface resistivity distributions of soil and rocks. Resistivity is a fundamental physical parameter that reflects the ability of the subsurface materials to conduct electrical current, which is influenced by lithology, porosity, water content, salinity, and the presence of contaminants. Low resistivity typically indicates high ionic concentration or saturated zones, while high resistivity is associated with dry, compact, or coarse-grained materials (Ahmed & Sulaiman, 2001). In this study, the geoelectrical method was applied using a configuration of 48 electrodes with 1-meter spacing to provide high spatial resolution at medium depths.

In addition to resistivity, several soil physicochemical parameters (pH, electrical conductivity (EC), total dissolved solids (TDS), and soil texture) were analyzed from agricultural, residential, and plantation areas. EC and TDS are closely related physical indicators that describe the concentration of dissolved ions in soil water, where high values may signal salinization or contamination. Soil pH governs chemical reactions within the soil and affects nutrient availability and ion mobility, while soil texture (percentages of sand, silt, and clay) influences porosity, permeability, and water retention capacity. These physical and chemical parameters were used to validate geoelectrical interpretations and provide a more robust understanding of the subsurface processes (Kotra et al., 2016).

Sukasari Village was chosen as the study area because it has considerable agricultural potential but also exhibits indications of declining groundwater quality in several locations. This degradation is suspected to result from the infiltration of agricultural inputs and domestic waste. By integrating geoelectrical data with soil physicochemical analysis, this study aims to identify zones suitable for agricultural activities while simultaneously detecting the risk of groundwater contamination. The objectives of this study are: (i) to determine variations in groundwater conditions in agricultural and residential areas through subsurface resistivity analysis, and (ii) to evaluate the physicochemical characteristics of soils from various land uses in the study area. The results are expected to provide valuable scientific information as a basis for planning and decision-making in the sustainable management of agricultural land and groundwater resources by both communities and policymakers.

2. METHODS

2.1 Research Methodology

This research was conducted in Sukasari Village, Sukasari District, Sumedang Regency. The geological map of Sukasari Village (Fig. 1) shows that the area is predominantly composed of volcanic rocks resulting from the relatively young volcanic activity of Mount Tangkuban Parahu and Mount Tampomas during the Quaternary period (Kusumadinata, 1979). The main lithological units include tuffaceous sand, lapilli, breccia, lava, and agglomerates, which shape a geomorphology of small plains and low hills influenced by volcanic deposition, erosion, and weathering processes. These volcanic materials, while producing fertile soils that support agriculture, also create geological hazards such as erosion and slope instability (Sukarman et al., 2020). Hydrogeologically, porous breccia and agglomerates function as groundwater reservoirs, whereas compact lava layers act as impermeable barriers that restrict groundwater flow (Arifianto et al., 2018; Irianto et al., 2024).

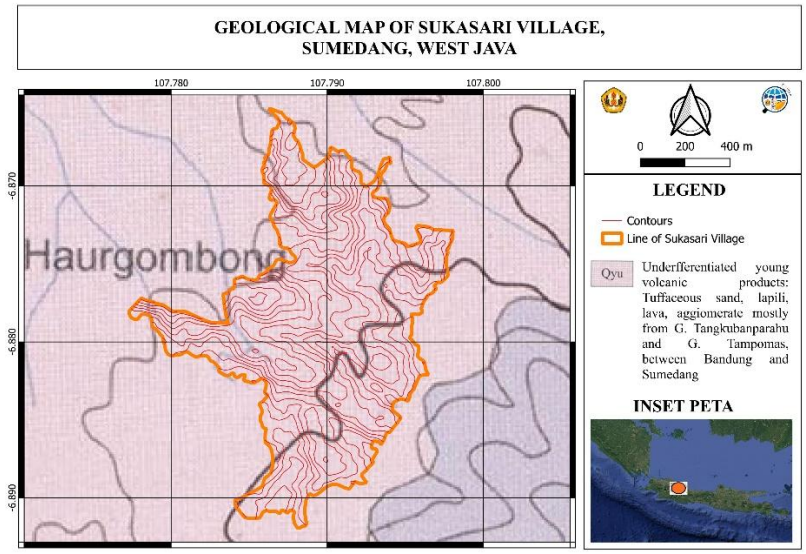

Figure 1. Geological Map of the Study Area

This research was conducted in sequential stages, beginning with a preliminary study to review literature and collect regional information. Base maps (geological) were then analyzed to select observation sites Fieldwork involved geoelectrical surveys and soil sampling across agricultural, residential, and plantation areas. Data were processed through geoelectrical inversion and laboratory analyses, followed by integrated interpretation to delineate contaminated zones and assess agricultural land suitability in Sukasari Village. The research methodology is illustrated in the following flowchart:

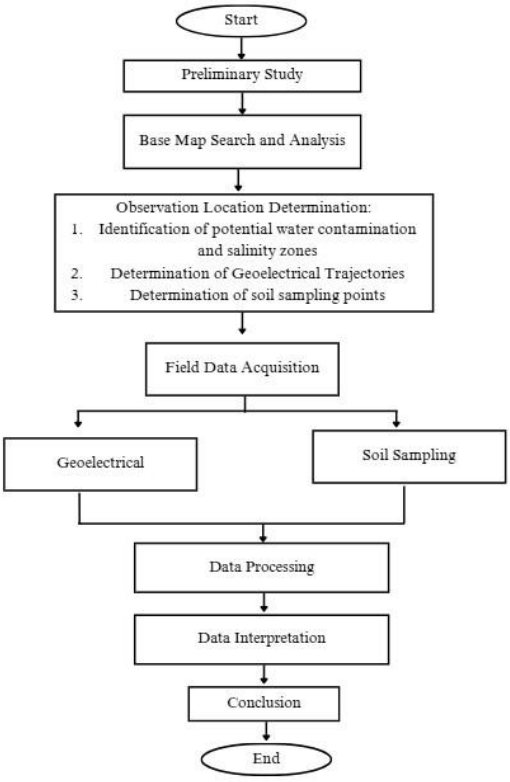

Figure 2. Research Flowchart

The geoelectrical survey was conducted from April 25 to 27, 2025, at three locations in Sukasari Village, Tanjungsari District, Sumedang Regency: the rice fields, the area in front of the biodigester, and the garden behind the biodigester (Fig. 3). The measurement points were distributed across eight survey lines within an area of approximately 8.77 hectares. The coordinates of each line are as follows:

1. Line 1 extends from −6.87555° S, 107.78526° E (southwest) to −6.87531° S, 107.78536° E (northeast).
2. Line 2 extends from −6.87568° S, 107.78546° E (east) to −6.87561° S, 107.78529° E (west).
3. Line 3 extends from −6.87567° S, 107.78552° E (south) to −6.87546° S, 107.78558° E (north).
4. Line 4 extends from −6.87559° S, 107.78551° E (southwest) to −6.87546° S, 107.78571° E (northeast).
5. Line 5 extends from −6.87744° S, 107.78557° E (northwest) to −6.87750° S, 107.78577° E (southeast).
6. Line 6 extends from −6.87703° S, 107.78594° E (west) to −6.87704° S, 107.78615° E (east).
7. Line 7 extends from −6.87621° S, 107.78511° E (northwest) to −6.87640° S, 107.78525° E (southeast).
8. and Line 8 extends from −6.87611° S, 107.78512° E (west) to −6.87617° S, 107.78531° E (east).

Data acquisition was performed using the Marcapada resistivity meter with a Wenner configuration, chosen for its ability to provide stable and high-resolution resistivity data for shallow subsurface characterization.

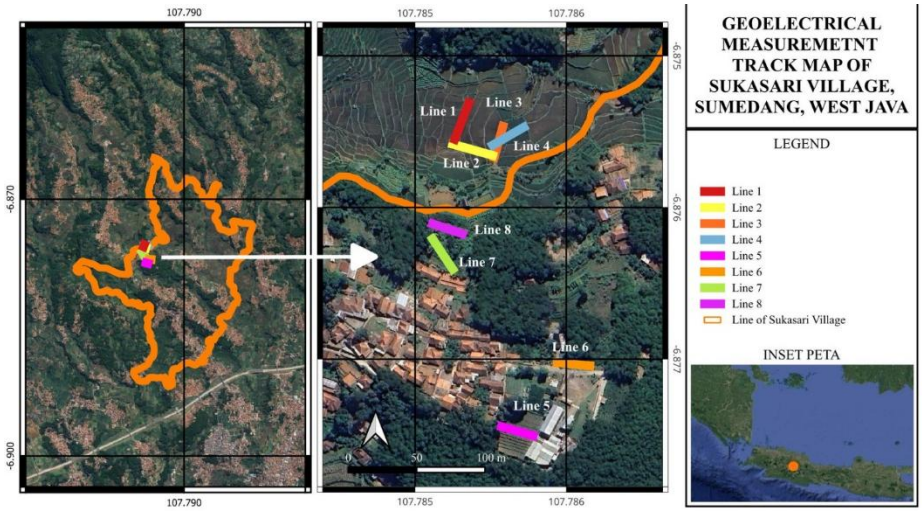

Figure 3. Geoelectrical Measurement Track Map

A total of eight survey lines were measured, comprising five lines with 0.5 m electrode spacing and three lines with 1 m spacing, each extending 48 m with 48 electrodes. Both spacings are considered small, optimized for detecting shallow subsurface contamination (<15 m) with varying resolution and depth sensitivity. The apparent resistivity data were processed using RES2DINV software applying the Least Squares Inversion technique, which iteratively minimizes the difference between observed and calculated apparent resistivity values to generate a smooth, realistic 2D resistivity model. This approach effectively delineates potential groundwater contamination zones and supports the interpretation of subsurface conditions in the agricultural and residential areas of Sukasari Village.

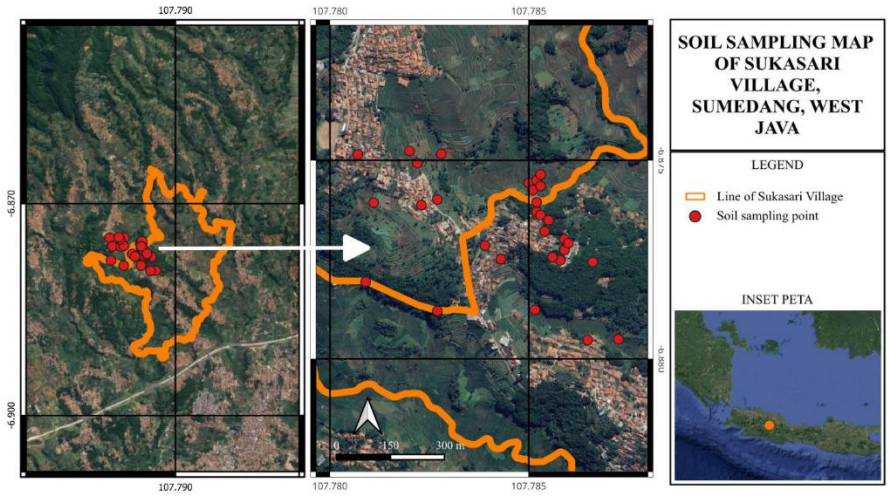

Figure 4. Soil Sampling Map

The sampling locations were determined based on the interpretation of the subsurface flow map, which illustrates the pathways of groundwater movement within the study area (Fig. 4). Sampling points were strategically selected along these flow paths to represent soil conditions influenced by groundwater dynamics. Additional considerations in site selection included accessibility and safety during field activities. Soil samples were collected directly in the field, with approximately 1 kilogram taken from each observation point. The samples were placed in pre-labeled plastic bags according to their location codes, then transported to the laboratory for further analysis.

3. RESULT AND DISCUSSION

3.1 Geoelectrical Method

Line 1 is situated within a rice field area at a lower elevation compared to the residential and plantation zones (Fig. 5). The near surface layer (Fig. 6) displays relatively homogeneous resistivity values ranging from 30 to 60 Ωm, which are characteristic of silty to clayey materials (Agustine et al., 2023) At a distance of approximately 12 meters along the profile and depths between 1 and 3 meters, resistivity values markedly decrease to 4–16 Ωm, reflecting a high degree of water saturation associated with continuous irrigation in the paddy fields. Conversely, a zone of high resistivity (>100 Ωm) is identified in the lower-left portion of the profile, suggesting possible contamination by pesticide residues or other anthropogenic inputs transported from the higher residential and plantation areas (Putri et al., 2024). These high resistivity anomalies spatially correspond to Lines 7 (Fig. 18) and 8 (Fig. 20) indicating potential downslope migration of pollutants from the southwest south sectors following both surface and subsurface water pathways, ultimately accumulating in the rice field area and contributing to the observed resistivity heterogeneity.

Figure 5. Field Conditions of Geoelectrical Acquisition Line 1

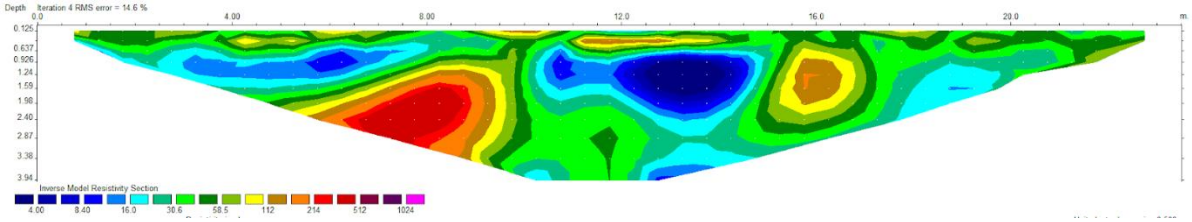

Figure 6. Field Conditions of Geoelectrical Acquisition Line 1 and Geoelectrical Cross Section of Line 1 Measurement

Line 2 is located in a rice field area at a lower elevation than the surrounding residential and plantation areas (Fig. 7), making it a potential site for water accumulation. The surface layer (Fig. 8) shows relatively homogeneous resistivity values of 30–60 Ωm, although some variations occur with both higher and lower resistivity values. These variations are likely influenced by local factors such as soil compaction due to agricultural activities or fertilizer application. In addition, indications of contamination are observed in zones of higher resistivity, although the intensity is not as pronounced as in Line 1. This suggests that contamination from the surrounding areas has reached Line 2, but its impact remains relatively minor.

Figure 7. Field Conditions of Geoelectrical Acquisition Line 2

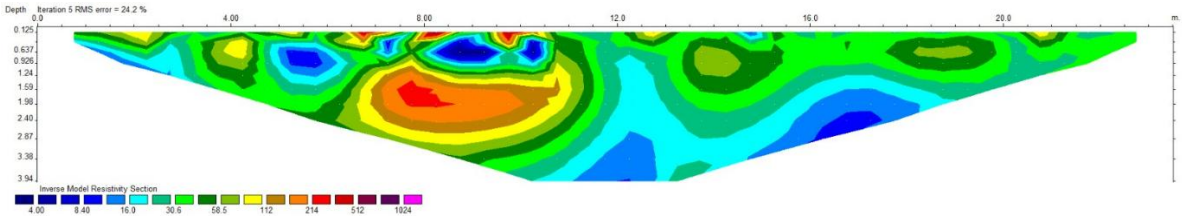

Figure 8. Geoelectrical Cross Section of Line 2 Measurement

Line 3 exhibits distinct resistivity characteristics (Fig. 9). The surface layer (Fig. 10) shows moderate resistivity values (30–100 Ωm), likely resulting from burning activities in the rice field area that caused surface soils to dry. At depths greater than 2 meters, resistivity decreases, indicating the presence of substantial groundwater reserves despite the dry surface conditions. No high-resistivity anomalies were observed that could suggest contamination, implying that the subsurface in this area remains relatively uncontaminated.

Figure 9. Field Conditions of Geoelectrical Acquisition Line 3

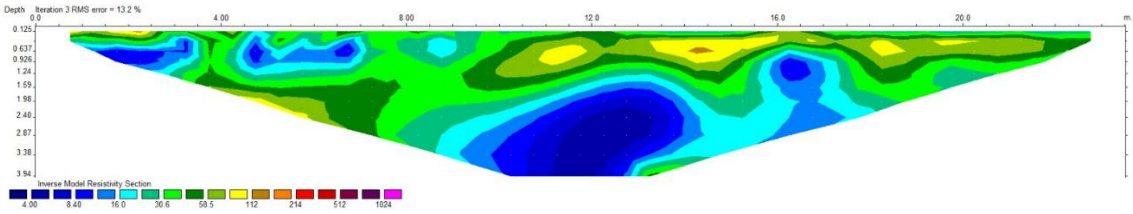

Figure 10. Geoelectrical Cross Section of Line 3 Measurement

Line 4 shows similar features. The surface soil appears dry due to rice field burning activities (Fig. 11), as indicated by moderate resistivity values (30–100 Ωm) in Figure 12. At approximately 2 meters depth, resistivity decreases, confirming the presence of significant groundwater reserves below the surface. This suggests that surface dryness does not markedly affect deeper subsurface conditions. Additionally, no high-resistivity anomalies were detected, indicating that the soil and groundwater quality in this section is relatively preserved.

Figure 11. Field Conditions of Geoelectrical Acquisition Line 4

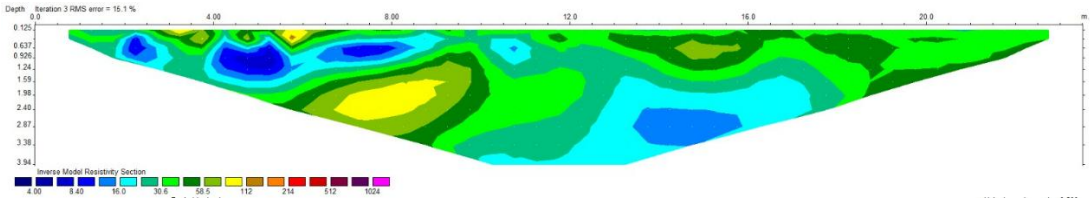

Figure 12. Field Conditions of Geoelectrical Acquisition Line 4

Line 5 is located in a young tobacco plantation area (Fig. 13), situated near a biodigester facility, which functions to process organic waste into biogas as well as liquid and solid fertilizer (Artiani & Handayasari, 2017). Given its proximity, this line was initially assumed to exhibit the highest contamination levels. However, the results shown in Figure 14 indicate that the surface layer down to a depth of approximately 90 cm has a dominant resistivity of 30–60 Ωm, which is still consistent with the typical characteristics of plantation soils. A localized low-resistivity anomaly (thickness 2 m) was identified at points 22–31, suggesting ion accumulation likely derived from accumulation of dissolved ions. Overall, the results show only limited and localized contamination, contrary to the initial assumption of severe impact from the biodigester.

Figure 13. Field Conditions of Geoelectrical Acquisition Line 5

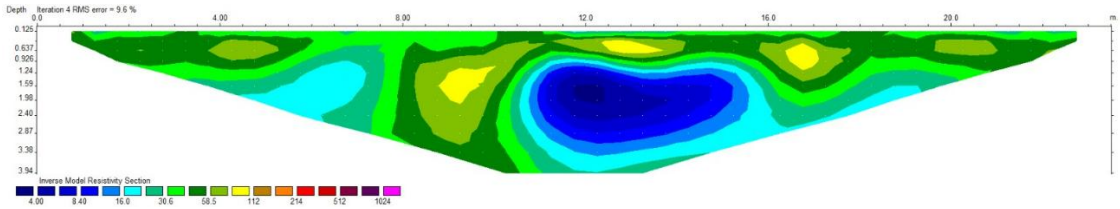

Figure 14. Field Conditions of Geoelectrical Acquisition Line 5

Line 6 is located between the biodigester and the paddy fields to the north, at a lower elevation that naturally directs flow from the biodigester toward the settlements and agricultural areas (Fig. 15). At points 1–13 in Figure 16, dominated by grassland, the surface resistivity is relatively homogeneous (30–60 Ω). However, at a depth of around 2 meters, higher resistivity values appear, likely associated with the accumulation of contaminants from domestic waste or biodigester runoff. Meanwhile, at points 14 to the end of the line, within plantation areas, surface resistivity tends to be lower, but at depths of 0.8 and 1.5 meters, a significant increase up from 100 Ωm is observed, indicating the possible use of pesticides or agricultural chemicals (Agustine et al., 2023). Overall, the resistivity pattern along Line 6 reflects the combined influence of local agricultural activities and potential waste flow from the biodigester.

Figure 15. Field Conditions of Geoelectrical Acquisition Line 6

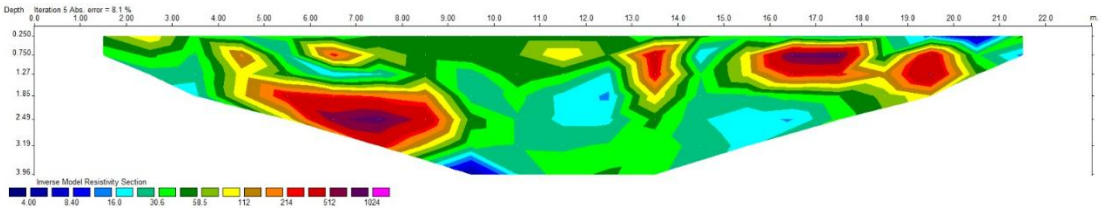

Figure 16. Field Conditions of Geoelectrical Acquisition Line 6

Line 7 is situated in a plantation area at an elevation between the residential zone and the rice fields (Fig. 17), serving as a natural pathway for wastewater flow from the settlement toward the fields. The surface layer, approximately 50 cm thick (Fig. 18), exhibits resistivity values of 30–60 Ωm, suggesting the predominance of silty soils. At a depth of around 2 meters, higher resistivity values (from to 100 Ωm) are observed, which may indicate the accumulation of pollutants from residential waste transported by surface runoff and deposited below the surface. Meanwhile, at points 5–6, a low

resistivity zone is detected, reflecting wetter soil conditions likely influenced by agricultural activities in the surrounding plantation area.

Figure 17. Field Conditions of Geoelectrical Acquisition Line 7

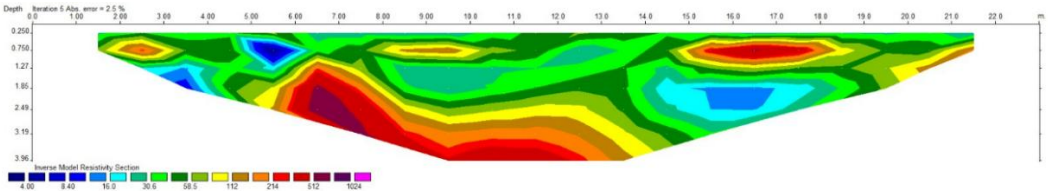

Figure 18. Field Conditions of Geoelectrical Acquisition Line 7

Line 8 is located in an area with dense vegetation, positioned between the residential zone and the rice fields (Fig. 19), serving as a pathway for wastewater flow from the settlement toward the fields. The surface layer, approximately 1 meter thick (Fig. 20), exhibits resistivity values of 30–60 Ωm, indicating the predominance of silty and clayey soils. At depths around 2 meters, higher resistivity values (100–300 Ωm) are observed, which may reflect the accumulation of pollutants from residential waste at deeper subsurface levels. Correlation with Line 7 suggests that this area is notably impacted by contamination starting below 2 meters depth.

Figure 19. Field Conditions of Geoelectrical Acquisition Line 8

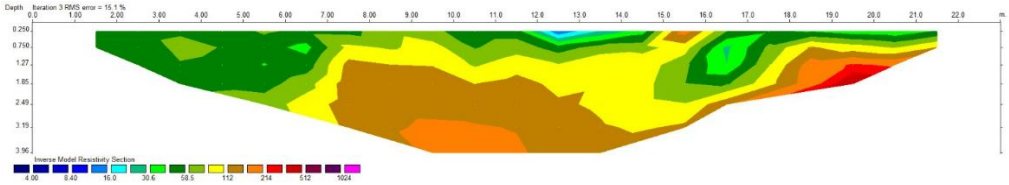

Figure 20. Field Conditions of Geoelectrical Acquisition Line 8

Overall, this study revealed subsurface resistivity variations of 4–1000 Ωm, reflecting diverse soil and groundwater conditions influenced by agricultural, residential, and biodigester activities. Low resistivity zones (4–16 Ωm) in Lines 3–4 indicate high soil saturation, while moderate values (30–60 Ωm) in most surface layers represent silty to clayey soils. Localized high resistivity anomalies (>100 Ωm) in Lines 1 and 2 and 6 until 8 suggest contaminant accumulation or chemical use in plantations. Beyond the technical results, these findings provide valuable insights for geoscience education, offering a real-world example that links resistivity concepts with environmental conditions and supports student learning in data interpretation, inversion modeling, and sustainable groundwater studies.

3.2 Soil Sampling Method

Soil sampling measurements are also carried out by looking at 5 physical and chemical parameters, namely soil texture, pH, EC, TDS as shown in table 1 below

Table 1. Physical and Chemical Parameters Data in Fields, Residential Areas, and Plantations

Name	Longitude	Lattidude	Soil Texture	pH	EC	TDS
Fields 1	807805.4	9239110	Loamy Sand	6	0.05	43
Fields 2	807827.6	9239118	Loamy Sand	5.5	0.03	30
Fields 3	807816.4	9239090	Loamy Sand	6	0.02	25
Fields 4	807838.6	9239101	Loamy Sand	6	0.02	22
Fields 5	807839	9239133	Sand	5.5	0.07	54
Fields 6	807562.6	9239193	Loamy Sand	6.5	0.03	18
Fields 7	807821	9238756	Loam	5.5	0.05	44
Fields 8	808052.4	9238673	Sand	6	0.03	33
Residential 1	807330.3	9239192	Sandy Loam	5.5	0.08	66
Residential 2	807506.4	9239050	Sand	6.5	0.01	13

Residential 3	807682.7	9238936	Loamy Sand	6	0.06	51
Residential 4	807726.8	9238898	Sandy Loam	6	0.09	70
Residential 5	807967.2	9238671	Clay Loam	5.5	0.05	47
Plantations 1	807496	9239167	Sand	6.5	0.02	12
Plantations 2	807474.1	9239201	Loamy Sand	6	0.02	24
Plantations 3	807373.7	9239057	Loamy Sand	5.5	0.04	27
Plantations 4	807550.8	9239065	Sand	6	0.01	11
Plantations 5	807827.2	9239056	Sandy Loam	6.5	0.01	7
Plantations 6	807827.1	9239029	Sandy loam	6	0.01	11
Plantations 7	807827	9239023	Sand	5.5	0.07	19
Plantations 8	807827	9239023	Sandy loam	5.5	0.07	57
Plantations 9	807838.1	9239020	Sandy loam	5.5	0.08	64
Plantations 10	807860.1	9239006	Loamy Sand	5.5	0.05	64
Plantations 11	807848.9	9238975	Sand	5.5	0.16	124
Plantations 12	807904.1	9238953	Sandy loam	5.5	0.05	47
Plantations 13	807915	9238941	Loam	6.5	0.01	10
Plantations 14	807922.1	9238941	Loam	6	0.01	20
Plantations 15	807929	9238946	Sandy Loam	6	0.01	12
Plantations 16	807903.9	9238923	Sandy Loam	6	0.07	61
Plantations 17	807870.6	9238905	Sandy Loam	6	0.07	56
Plantations 18	807870.6	9238903	Clay Loam	6.5	0.03	30
Plantations 19	807892.7	9238897	Loamy Sand	6.5	0.03	32
Plantations 20	807892.7	9238894	Sandy Clay Loam	6.5	0.05	43
Plantations 21	807982.6	9238889	Loamy Sand	6	0.01	17
Plantations 22	807548.9	9238754	Loamy Sand	5.5	0.02	26
Plantations 23	807350.3	9238837	Sand	6	0.01	12

Soil texture is a fundamental property that influences water retention, drainage, and nutrient availability. In this study, soil samples from Sukasari Village were analyzed to determine their textural composition and evaluate the implications for land use and management at each location, as presented in Figure 21.

a. Fields:
   The fields in Sukasari are generally characterized by Loamy Sand and Sand texture classes, resulting in well-drained soils with relatively low water and nutrient retention
b. Residential Areas:
   Across the five residential locations, soil textures are dominated by Sandy Loam and Loamy Sand in Residential 1, 3, and 4, indicating the influence of sandstone weathering. Residential 2 exhibits a Sand texture, while Residential 5 has a Clay Loam texture.
c. Plantations:
   The 23 plantation soil samples in Sukasari exhibit a wide range of texture classes, including Sand, Loamy Sand, Sandy Loam, Loam, Clay Loam, and Sandy Clay. The sand dominance reflects the influence of sandstone and young volcanic deposits, whereas the clay content indicates micro-geological controls and topographic conditions affecting drainage and fine particle sedimentation.

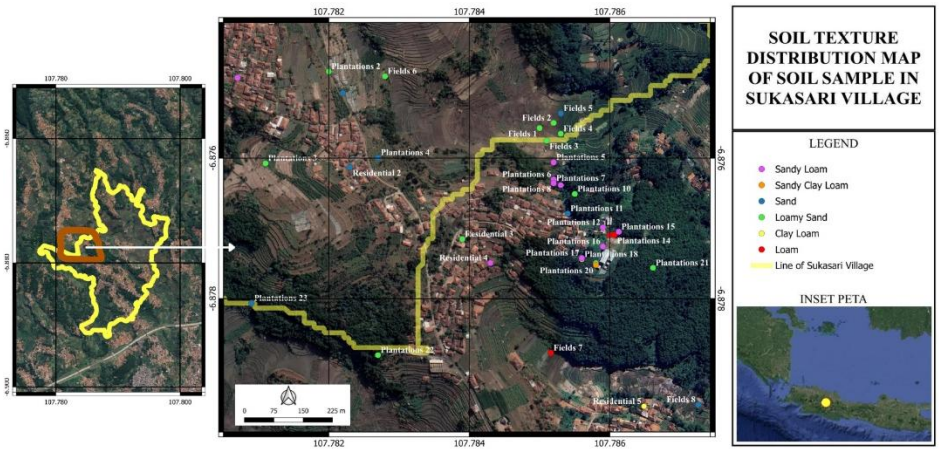

Figure 21. Soil Texture Distribution Map in Fields, Residential Areas, and Plantations of Sukasari Village

The soil pH values in the study area range from 5.5 to 6.5, as shown in Figure 23, indicating slightly acidic conditions. In the field areas, this acidity is influenced by the anaerobic decomposition of organic matter in waterlogged soils, which produces acidic compounds, along with the moist and low-oxygen conditions that promote the formation of reductive compounds (Hardjowigeno, 2003). In the residential areas, pH values are similar, but variations can be attributed to anthropogenic activities, such as domestic waste disposal and the use of construction materials, which affect soil structure and release H^+ions (Kasifah, 2017). Meanwhile, in the plantation areas, pH tends to remain stable due to the presence of vegetation and root activity, which release basic cations (Ca^{2+} and Mg^{2+}) through natural decomposition processes, thereby helping to maintain soil acidity balance.

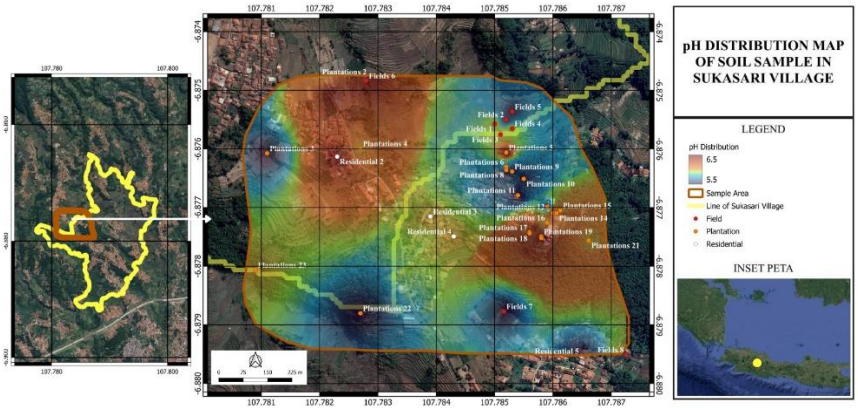

Figure 22. pH Distribution Map at Fields, Residential, and Plantation Locations in Sukasari Village

Soil Electrical Conductivity (EC) values in the study area showed variations across different land uses. In the fields, EC ranged from 0.02-0.07 dS/m, reflecting moist soil conditions with moderate dissolved salt content. These values are influenced by the irrigation system, which promotes the accumulation of ions such as Na^+, K^+, and Ca^{2+}, as well as redox processes in waterlogged soils, resulting in relatively stable conductivity consistent with the managed wetland function of the Fields (Rakhmawati et al., 2017). In residential areas, EC varied between 0.01-0.09 dS/m, influenced by anthropogenic activities such as waste disposal, construction, and surface modification. Meanwhile, plantation areas exhibited a wider EC range of 0.01–0.16 dS/m, with the highest values observed at

Plantation site 11, likely associated with intensive fertilization practices and the accumulation of organic matter that enriches dissolved ions in the soil.

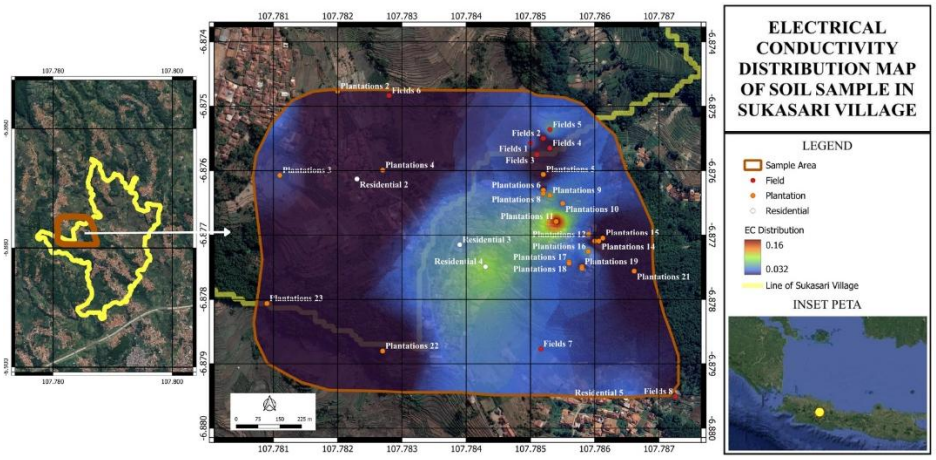

Figure 23. Map of EC Distribution in Fields, Residential, and Plantation Areas of Sukasari Village

The Total Dissolved Solids (TDS) values in the study area exhibit significant variation across different land-use types. In the fields, TDS ranges from 18-54 mg/L, with an average of 33.6 mg/L, which falls into the low to moderate category. This is influenced by the irrigation system that regularly wets the soil, causing leaching of dissolved ions such as Na^+, Ca^{2+}, Cl^-, and NO_3^-, which prevents the accumulation of solutes (Zheng et al., 2021). In residential areas, TDS ranges from 13-70 mg/L, with an average of 49.4 mg/L. This variation reflects differences in human activity intensity and water management practices. The higher values (66–70 mg/L) are likely associated with household waste contamination, septic tank leakage, or residual construction materials (Kasifah, 2017). Meanwhile, in the plantation areas, TDS ranges from 7-124 mg/L, with an average of 34.3 mg/L. The highest value (124 mg/L at Plantation site 11) is suspected to result from intensive fertilizer use or the decomposition of organic matter. Plantations receiving additional artificial nutrients tend to exhibit higher TDS compared to those relying solely on natural soil fertility.

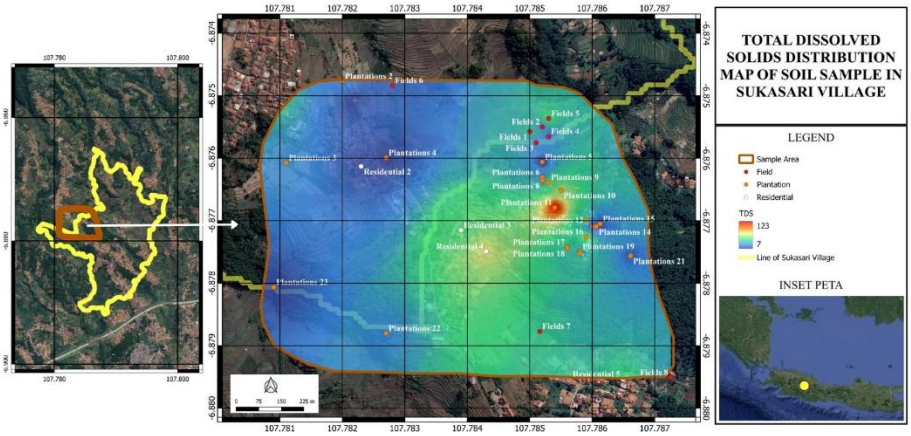

Figure 24. Distribution Map of Total Dissolved Solids (TDS) at Fields, Residential, and Plantation Locations in Sukasari Village

4. INTEGRATION OF GEOLELECTRICAL AND SOIL SAMPLING

Based on the integration of geoelectrical resistivity data and soil physicochemical parameters, the contamination hotspot is identified around Plantation site 11. The correlation matrix shows a strong

positive relationship between resistivity and both EC (r = 0.86) and TDS (r = 0.85), as well as a strong negative correlation with pH (r = –0.80). This indicates that areas with high resistivity values tend to exhibit higher electrical conductivity and total dissolved solids, along with more acidic conditions. At Site 11, physicochemical data confirm this trend, with a high TDS (124 mg/L), elevated EC (0.16 dS/m), and low pH (5.5).

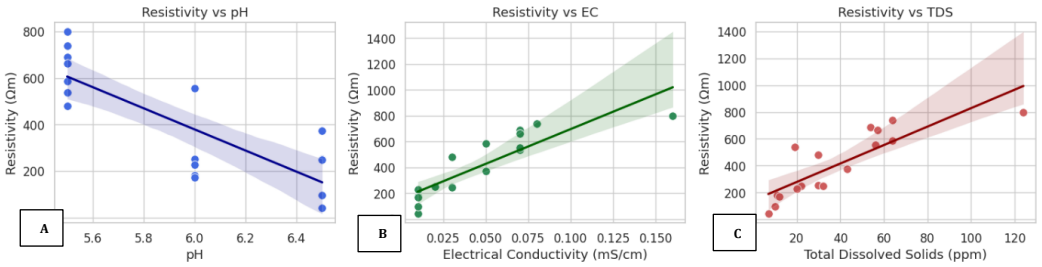

Figure 25. Scatter plots of (a) resistivity and pH, (b) resistivity and EC, and (c) resistivity and TDS

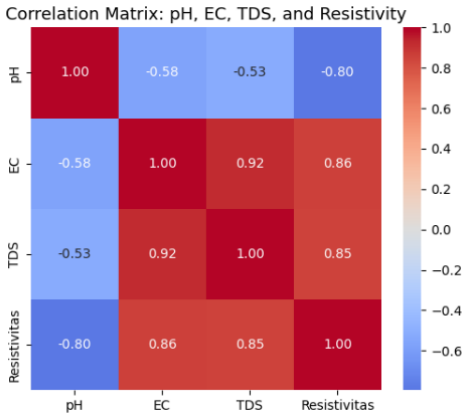

Figure 26. Correlation heat map between resistivity and soil physicochemical parameters

The soil texture in Plantation site 11 dominated by sandy loam, sand, and loamy sand—has high permeability, promoting infiltration of dissolved ions from waste sources into the subsurface. Geoelectrical survey results also reveal elevated resistivity values east and slightly north of Plantation 11. Considering the water flow direction and local topography, contaminants from this site are likely migrating toward the rice fields to the north. This is supported by the resistivity profiles (Lines 1 and 2), where high-resistivity anomalies correspond to the potential accumulation zones of dissolved contaminants. The integration between resistivity and soil sampling data thus strengthens the interpretation that contaminant transport and accumulation are closely linked to both geoelectrical signatures and soil physicochemical behavior.

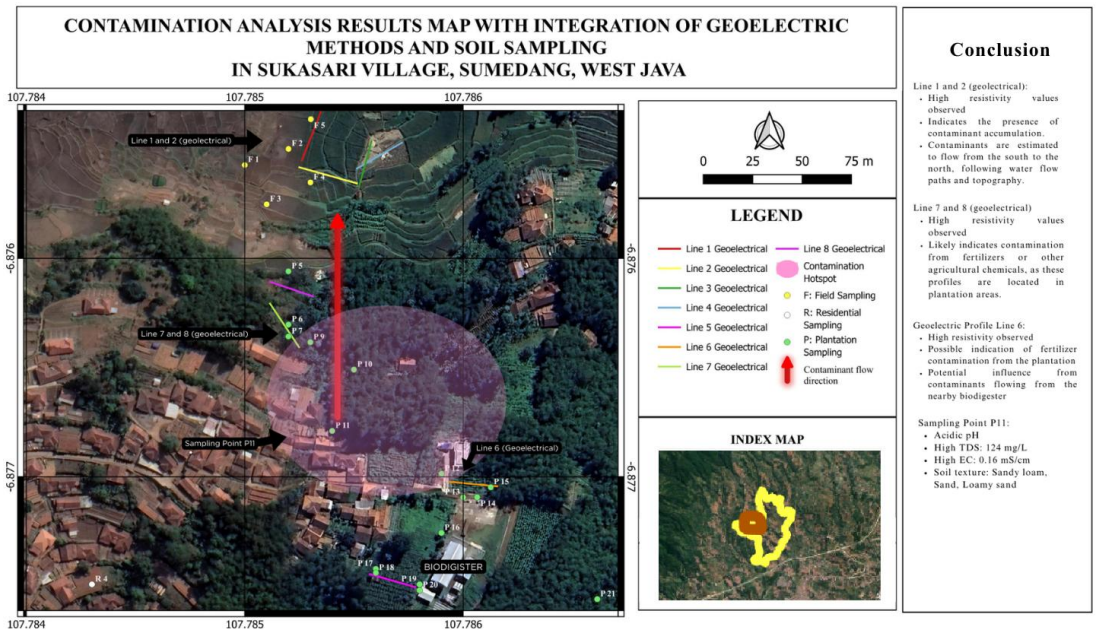

Figure 27. Contamination Analysis Results Map with Integration of Geoelectrical Methods and Soil Sampling

5. CONCLUSION

The integration of geoelectric surveys with soil physicochemical analyses effectively delineated both contamination zones and agriculturally suitable areas in Sukasari Village. Elevated contamination levels were identified primarily around plantation and residential zones, influenced by agrochemical inputs, domestic wastewater, and the high permeability of sandy–loamy soils that facilitate downward and lateral migration of dissolved constituents. These spatial patterns underscore the combined influence of land use, anthropogenic activities, and local topographic gradients on subsurface fluid pathways.

From a physics perspective, this study contributes to the advancement of applied geophysics by reinforcing the role of electrical resistivity as a fundamental physical parameter for subsurface characterization. The observed correlations between resistivity and key physicochemical variables—such as ionic concentration (EC and TDS), pH, and moisture content—provide empirical support for electromagnetic conduction processes in heterogeneous porous media. By demonstrating how resistivity variations reflect changes in soil chemistry and fluid properties, the findings enhance the scientific basis for utilizing geophysical methods in groundwater quality assessment, environmental monitoring, and contamination studies.

REFERENCES

Agustine, E., Gunawan, N., Rifky Nauval, Muhammad Abdilllah Budianto, Irwan Ary Darmawan, Dini Fitriani, Kartika Hajar Kirana, Wahyu Srigutomo, Asep Harja, Imran Hilman Mohammad, & Eddy Supriyana. (2023). Land Suitability and Plant Types Based on Soil Electrical Properties and Remote Sensing. *Jurnal Geologi Dan Sumberdaya Mineral*, *24*(2), 89–96. https://doi.org/10.33332/jgsm.geologi.v24i2.723

Ahmed, A. M., & Sulaiman, W. N. (2001). Evaluation of groundwater and soil pollution in a landfill area using electrical resistivity imaging survey. *Environmental Management*, *28*(5), 655–663.

Arifianto, I., Palupi Savitri, K., Rachmat Fadhil Priana, M., & Setianto, A. (2018). *Groundwater exploration in volcanic morphology using geophysical schlumberger resistivity method, in Jeneponto, South Sulawesi Province*.

Artiani, G. P., & Handayasari, I. (2017). Optimalisasi pengolahan sampah organik dengan teknologi biodigester sebagai upaya konservasi lingkungan. *Jurnal Kajian Ilmu Dan Teknologi*, *6*(2), 95–105.

Brontowiyono, W., Asmara, A. A., Jana, R., Yulianto, A., & Rahmawati, S. (2022). Land-Use Impact on Water Quality of the Opak Sub-Watershed, Yogyakarta, Indonesia. *Sustainability (Switzerland)*, *14*(7). https://doi.org/10.3390/su14074346

Hardjowigeno, S. (2003). Ilmu Tanah. Akademika Pressindo, jakarta. Retrieved from. *Perpus. Wiraraja. Ac. Id/Opac/Index. Php*.

Irianto, S., Kusumayudha, S. B., Prasetyadi, C., & Yatini, Y. (2024). Analysis of the potential of volcanic aquifers in supporting the development of groundwater resources in Bogor District, West Java. *OPSearch: American Journal of Open Research*, *3*(6), 114–129. https://doi.org/10.58811/opsearch.v3i6.114

Kasifah, K. (2017). *Dasar-Dasar Ilmu Tanah*. Fakultas Pertanian, Universitas Muhammadiyah Makasar.

Kotra, K. K., Yedluri, I., Prasad, S., & Pasupureddi, S. (2016). Integrated Geophysical and Geochemical Assessment for the Comprehensive Study of the Groundwater. *Water, Air, and Soil Pollution*, *227*(6). https://doi.org/10.1007/s11270-016-2902-3

Kusumadinata, K. (1979). Data Dasar Gunungapi Indonesia. In *Catologue of References on Indonesian Volcanoes with Eruptions in Historical Times, Volcanol Surv Indonesia* (pp. 178–179).

Putri, B. A., Putri, A. S. N., Prameswary, C. A., Ekklesia, E., Donita, F. T., Rahmawati, N., Agustine, E., & Susilawati, A. (2024). Identification of Pesticide-Saturated Soil Using Near-Surface Geophysics Method. *Jurnal Phi: Jurnal Pendidikan Fisika Dan Fisika Terapan*, *10*(1), 28–34.

Rakhmawati, L. A., Agustine, E., Fitriani, D., & Hasanah, M. U. (2017). Prosiding Seminar Nasional Fisika (E-Journal) SNF2017 Seminar Nasional Fisika 2017 Prodi Pendidikan Fisika dan Fisika, Fakultas MIPA. *Prosiding Seminar Nasional Fisika (E-Journal) SNF2017*, *VI*. https://doi.org/10.21009/03.SNF2017

Sukarman, S., Dariah, A., & Suratman, S. (2020). TANAH VULKANIK DI LAHAN KERING BERLERENG DAN POTENSINYA UNTUK PERTANIAN DI INDONESIA / Volcanic Soils in Sloping Dry Land and Its Potential for Agriculture in Indonesia. *Jurnal Penelitian Dan Pengembangan Pertanian*, *39*(1), 21. https://doi.org/10.21082/jp3.v39n1.2020.p21-34

Yusuf, W. A., Susilawati, H. L., Wihardjaka, A., Harsanti, E. S., Adriany, T. A., Dewi, T., Pramono, A., Kurnia, A., Ferry, I., & Al Viandari, N. (2023). *Kerusakan dan pencemaran lingkungan pertanian: karakteristik dan penanggulangannya*. UGM PRESS.

Zheng, N., Guo, M., Yue, W., Teng, Y., Zhai, Y., Yang, J., & Zuo, R. (2021). Evaluating the impact of flood irrigation on spatial variabilities of soil salinity and groundwater quality in an arid irrigated region. *Hydrology Research*, *52*(1), 229–240. https://doi.org/10.2166/NH.2020.209